Leaf Identification in High-Density LiDAR-RGB Data

Isabella Subtil Norberto[1], Clodoaldo Souza Faria Junior[1], Antonio Maria Garcia Tommaselli[1], Milton Hirokazu Shimabukuro[1], Rorai Pereira Martins-Neto[2], Nilton Nobuhiro Imai[1], Matheus Ferreira da Silva[1]

[1]Faculty of Science and Technology, São Paulo State University (UNESP) at Presidente Prudente, São Paulo 19060-900, Brazil – (isabella.subtil, clodoaldo.souza, a.tommaselli, milton.h.shimabukuro, nilton.imai, matheus-ferreira.silva)@unesp.br
[2]Faculty of Forestry and Wood Sciences, Czech University of Life Sciences Prague (CULS), Kamycka 129, 16500 Prague, Czech Republic – pereira_martins_neto@fld.czu.cz

Keywords: terrestrial LiDAR data, colouring point cloud, leaf segmentation, spectral identification, precision agriculture.

Abstract

Leaf detection through automated segmentation of 3D data is becoming a crucial technique in many applications of digital agriculture. Some 3D segmentation techniques that can be mentioned are based on normal differences and median normalised vector growth. However, applying these approaches to high canopy density data remains challenging. In this study, we propose a processing flow for leaf detection in high canopy density LiDAR-RGB point clouds. First, a noise removal technique inspired by Moving Least Squares (MLS) was applied to the LiDAR point cloud, and a RGB colour was assigned to each point by combining computer vision and photogrammetric methods. Moreover, once the data were suitable for leaf detection, the branches were filtered using the Statistical Outlier Removal (SOR) filter based on an analysis of the statistical behaviour of the neighbourhood. Afterwards, an unsupervised DBSCAN (Density-Based Clustering Non-Parametric Algorithm) method was used to segment similar points. Finally, the points within each cluster were identified as leaf or non-leaf using the RGB values implemented by our method; ground points were filtered out using a maximum height threshold. As a result, the leaf, non-leaf, and ground point identifiers were correct in 98.9% of cases, with the branch filtering technique SOR proving effectiveness in removing branches with low information loss and without additional complex point densification steps in reconstruction. This SOR-based solution overcomes major challenges in semantic segmentation (leaves and branches) in high-density data and potentially contributes to precision agriculture.

1. Introduction

Leaves compose the primary surface of vegetation and play a vital role in photosynthesis and respiration, which are essential for plant life. Quantification of leaves on trees is a common task in plant phenotyping, particularly with the automatic segmentation of branches and leaves in digital data. This quantification is an essential prerequisite for extracting phenotypic traits, such as height, density, biomass and quantitative parameters regarding plant complexity (Li et al., 2020). For example, the Leaf Area Index (LAI) serves as a key parameter for estimating biomass. Leaf segmentation facilitates LAI estimation based on leaf point distribution around the stem or branches (Masuda, 2021). Moreover, it enables the modelling of photosynthetic studies (Li et al., 2017) and the quantification of plant architecture (Li et al., 2022). Previously, manual measurement of phenotypic traits was a costly, error-prone process, and environmentally damaging (Jin et al., 2018). Nevertheless, identifying and separating tree elements allows for studying leaf aspects and root morphology (Costa et al., 2019).

The advancement of image-based methods has significantly boosted the extraction of high-throughput phenotypic traits. However, reconstructing three-dimensional images does not guarantee high accuracy and may lose crucial spatial and volumetric information under field conditions. Terrestrial Laser Scanners (TLS) have been used in precision agriculture, offering fast, non-destructive, and accurate techniques for high-yield crops (Jimenez-Berni et al., 2018). Combining images and TLS-derived point clouds is advantageous in segmentation by delivering high-quality spatial and spectral information through data fusion. Dorj et al. (2017) developed a technique for citrus fruit yield estimation based on colour features through data segmentation. Point cloud segmentation technology is widely employed for preprocessing 3D point cloud data of plants in forestry and agriculture. This technique enables the grouping and segmentation of individual elements or plant organs, facilitating a more detailed analysis of plant structure (Hu et al., 2022).

Tree segmentation is a topic of relevance, explored both in forest ecology and digital agriculture. In forest ecology, the importance of distinguishing tree elements at different scales, such as trunk, branches, and leaves, is highlighted. This approach commonly employs point-to-point classification strategies in most wood-leaf separation methods (Wan et al., 2021), due to scale variation. In digital agriculture, recent studies have focused on medium and small-sized trees, with a particular emphasis on distinguishing stems and leaves. TLS technology has been used due to its ability to separate diverse geometric features, such as leaves, branches, trunks, and stems. Studies in forest ecology, such as mentioned by Zhou et al. (2019), concluded that multiscale methods are effective for this challenge.

In precision agriculture, the differences in plant structures are generally less evident, simplifying segmentation. Techniques such as segmentation based on normal differences (Li et al., 2017) or the application of the median normalised vector growth method (Jin et al., 2018) have shown promising results. However, these techniques can be further refined with machine learning algorithms to segment stems and leaves in real field environments, as proposed by Ao et al. (2022). Gomes and Zheng (2020) investigated data augmentation techniques, such as the use of Generative Adversarial Network, for leaf segmentation and counting. Li et al. (2018) proposed an approach for segmenting individual leaves using over-segmentation and region growing in greenhouse ornamental plants. However, applications in real field environments with high canopy density data, especially in shrub-like trees, are still limited.

In summary, the following contributions are proposed:
• A strategy for leaf segmentation with less complex methodologies.
• An approach for clustering leaves, non-leaf, and ground points.

https://doi.org/10.5194/isprs-annals-X-3-2024-269-2024

• A procedure for data labelling based on colour features extracted from the coloured point cloud.
• Experiments and discussions on the potential of the proposed methodologies to improve existing techniques.

2. Background

2.1 Terrestrial LIDAR data initial processing

2.1.1 Noise Filtering

Noise caused by different sources, such as airborne dust, insects, and air humidity, is common during field surveys with TLS instruments (Hu et al., 2022). There are also natural causes that can distort object representation, such as wind on leaves and incident sunlight. Another relevant error source is the instrument settings, which can lead to the creation of outliers due to increased resolution and quality, resulting in the accumulation of measurements at the same point during acquisition, creating multiple layers. The data quality can be improved by removing noise and facilitating the following processing steps.

Statistical filters can be a good option for noise removal in point clouds. The statistical technique called Moving Least Squares (MLS) is mentioned as being capable of preserving the characteristics of irregular data (Schall et al., 2005), such as leaves and branches. Jenke et al. (2006) define MLS as a smoothing process over a point cloud by locally fitting polynomials to individual points while simultaneously computing the normal for each smoothed point.

2.1.2 Assigning spectral values to points

Real scenes can be reconstructed in three dimensions with colour and texture information by fusing Light Detection and Ranging (LiDAR) data with spectral information acquired by an optical camera (Seitz and Dyer, 1999). The generation of these coloured point clouds requires the integration of RGB or multispectral cameras to the TLS. Data fusion requires the determination of the camera locations and orientation with respect to the LiDAR point cloud reference system. Crombez et al. (2015) described the projection of the data based on estimates of interior and exterior camera orientations with respect to the point cloud. Although TLS with narrow beam divergence can penetrate dense vegetation, the resulting point cloud still suffer from occlusion. The main data fusion challenges are occluded areas and double mappings, which are resolved by generating a visibility map.

Some relevant techniques for the generation of visibility mapping are Z-buffer (Catmull, 1974), Binary Space Partitioning (Fuchs et al., 1980), Ray Casting (Appel 1968), Ray Tracing (Whitted, 1979) or Hidden Points Removal (HPR) (Katz et al., 2007). Additionally, culling algorithms such as Backface Culling (Blinn, 1993), Viewing Frustum Culling (Assarsson and Moller, 2000) or Occlusion Culling (Cohen-Or et al., 2003) can be used to restrict the view to the camera coverage. Seitz and Dyer (1999) studied the problem of point-cloud colouration and considered introducing a visibility restriction by identifying voxels with the same colour.

Currently, there exist machine learning methods capable of colouring a three-dimensional cloud. Liu et al. (2022) proposed the Point Cloud Colorization Network (PCCN) based on an Adversarial Generative Network to map colour information to the point cloud. Colouring a LiDAR point cloud provides a complete 3D description, generating a virtual representation of real objects and elements in the environment for manipulation and analysis.

2.2 Branch filtering techniques

Difference of Normals (DoN) is a technique commonly used to discriminate different surfaces like tables and walls. However, researchers have recognised the potential of this technique to filter stems (Li et al. 2017). The method treats each leaf as a set of points lying on a plane, and the stem or branches as irregular or non-flat surfaces. Thus, the set of neighbouring normals can be used to distinguish them. Especially for trees with low canopy density, the results are promising, but at the cost of reducing the number of leaf points, as shown by Li et al. (2020). In this case, additional complex point densification steps are still required to reconstruct the leaves.

An alternative is to explore statistical filtering methods to remove branches on leaves by treating them as outliers. Statistical Outlier Removal (SOR) filter, combined with a neighbourhood radius, has been mentioned to be efficient for noise removal in LiDAR point clouds. SOR assumes that the distance between a point and its neighbours follows a normal distribution (Zhang, 1994). The average distance is calculated considering the K nearest neighbours (KNN) for each point in the dataset. This method was previously applied for the removal of spines on *Rosa roxburghii* (Xie et al., 2021), for the removal of outliers near trees (Li et al., 2022), and for the removal of noise produced by rain and snowfall (Huang et al., 2023). The technique has the potential to remove clusters of points scattered between denser regions, typical of trees with dense foliage and small branches. Nevertheless, the filtering of leaves depends on the clustering of the points that describe the leaves.

2.3 Leaf segmentation and identification

Clustering is widely used in statistical analysis for object detection and segmentation, especially in machine learning, being classified as an unsupervised learning technique (Ester et al., 1996). DBSCAN (Density-Based Clustering Non-Parametric Algorithm) uses a density-based clustering approach, in which density in a given region is the attribute for the formation of clusters (Khan et al., 2014).

Liu et al. (2020) investigated the possibility of using DBSCAN combined with an R-CNN mask and achieved promising results in indoor collections, especially for smaller plants. However, the challenges increased significantly in outdoor environments with dense foliage. Segmentation and identification of fruits using spectral information from images were investigated by Dorj et al. (2017). The methodology converts the RGB image to HSV (Hue, Saturation and Value), thresholds it, and detects the orange colour of the fruit. A few years later, the technique was explored by Hu et al. (2022) to segment a LiDAR-RGB point cloud for the estimation of Colza leaves.

3. Materials and methods

3.1 Materials

3.1.1 Terrestrial Laser Scanner and Optical Camera

The LiDAR point cloud was acquired with the FARO Focus Premium TLS. Its main features are 360° x 300° FoV, with 0.3 mrad divergence, pulse duration of approximately 4 ns, wavelength of 1553.5 nm, designed to scan objects ranging from 0.5 to 70 m with 1 mm accuracy and 19 arcsec angular accuracy (vertical and horizontal). The FARO Focus also allows RGB colouring with the attached camera. However, it is possible to explore the use of colouring techniques for point clouds with other cameras, for instance, multispectral cameras. In this paper, the fusion with images collected by an Agrowing (Agrowing Development Team, 2020) multispectral camera is being assessed.

A special mount with six lenses and spectral filters is adapted to a Sony Alpha 7 IVR sensor, model ILCE-7RM4A, by Agrowing, allowing the generation of fourteen image bands. The spectral bands are captured simultaneously since each lens redirects the light to a specific part of the sensor (Tommaselli et al., 2020). In this paper, LiDAR point clouds were coloured with spectral values from bands 430nm (blue), 550nm (green), and 650nm (red). Future studies will assess the potential for incorporating the full set of fourteen spectral bands to the point cloud.

3.2 Methods

3.2.1 Field Data Acquisition

Field surveying and data acquisition involve: (1) the determination of reference point positions, (2) camera setup, (3) image acquisition in the planned exposure stations and (4) a single LiDAR scan. In the experiment presented in this paper, a single LiDAR scan was coloured with images acquired from different stations.

Data were collected at the Federal University of Uberlândia (UFU) coffee plantation, Monte Carmelo/MG campus. Some targets were placed over the coffee tree and on the ground (step 1). The images were then acquired at different exposure stations, varying height, planimetric base and convergence, with a suitable shutter speed (steps 2 and 3). Finally, a single scan was performed with the Faro TLS with 10,240 pt/360° (Step 4). With the previously described configurations, 4,082,965 points were collected. This point cloud was clipped to the area of interest with the CloudCompare software (Figure 1).

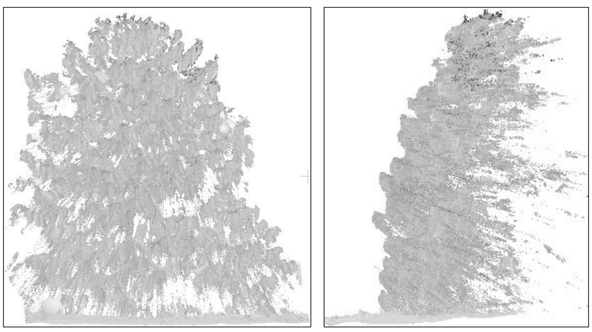

(a) (b)

Figure 1 – Clipped LiDAR point cloud (a) front and (b) side views.

Fifty images were acquired to cover the entire field of view corresponding to the scan of the LiDAR point cloud with the optical images. The next step was the extraction the image bands from each image using the AWBasic software and the processing of the LiDAR data using the FARO Scene software.

3.2.2 MLS

In this study, the MLS method implemented in PCL (Point Cloud Library) (Rusu and Cousins, 2011) was used for smoothing. The experiments performed in this paper were performed with the following settings for MLS algorithm: second-order polynomials for smoothing, utilising a KD-Tree search for efficient searching, and a surface smoothing radius of 1.8 mm.

3.2.3 Colourisation

Assigning spectral values to LiDAR cloud points, also known as colourisation, depends on the previous orientation of the camera images concerning the LiDAR point cloud reference system. Control points were identified, and their 3D coordinates were manually measured in the LiDAR cloud with Cloud Compare software. These points were then used for bundle adjustment (BA) in the Agisoft Metashape software. The Exterior and Interior orientation parameters (EOPs and IOPs) of the images were simultaneously determined with bundle adjustment (BA).

After estimating the IOPs of the camera lenses and the EOPs of each image, the point cloud is cropped using the VFC algorithm, using the EOPs of each image band. Cropping the point cloud will reduce the amount of data and the processing time of other methods avoiding the difficulties of dealing with dense datasets. Then, the points in the cloud that are occluded in the image are determined. In this methodology, the HPR technique (Katz et al., 2007) is applied to remove duplicate points and obtain leaves without overlap, adopting an approach similar to the work of Crombez et al. (2015).

Finally, the colourisation step assigns the spectral values to the LiDAR cloud points. Firstly, the 3D coordinates of a point are projected to the image using the collinearity equations. Then, the photogrammetric coordinates (x, y) are transformed to image coordinates (column, line) using inverse interior orientation; finally, the Digital Number (DN) to be assigned to the 3D point is interpolated from the neighbour’s pixels with bilinear interpolation. This process is repeated for all image bands and all 3D points visible from the camera station.

3.2.4 SOR

The SOR algorithm, originally designed for outlier removal, was used since the leaves have similar behaviour in terms of the magnitude of the average distances and the small standard deviations. LiDAR point cloud delineates leaves through geometric and dense clustering patterns, while branches are sampled with a lower point density. This makes it feasible to filter out the branches in the point clouds since the branches are considered outliers compared to the leaves’ behaviour. The filter needs to specify the quantity of neighbouring points within the clusters. The average distance between a point and its neighbours and the standard deviation of these points are analysed to filter out the outliers. To distinguish between branches and leaves in the point cloud, points are filtered out if they do not meet the specified criteria. Furthermore, an empirical study on the behaviour of the data was conducted considering different quantities of neighbouring points.

3.2.5 DBSCAN

DBSCAN is a non-supervised clustering method designed for analysis and data mining. This algorithm prioritises the density of points over other traditional methods, like k-means. One of the key advantages of DBSCAN is that it does not require the previous specification of the number of clusters, making it particularly useful when the underlying data structure is unknown. Instead, DBSCAN relies on two main parameters: tolerance and minimum points, which are required to consider a point as a central point. These parameters determined the neighbourhood size and the minimum density required for a point to generate a new cluster (Khan et al., 2014).

DBSCAN operates by identifying central points that have a minimum number of points within their neighbourhood, determined by the tolerance value, and then expands the clusters connected in their attainable neighbourhoods. Therefore, points that are not a central point and do not belong to the neighbourhood of any central point are considered noise (Deng, 2020).

The implementation of this algorithm utilised the Scikit-learn library (Pedregosa et al., 2011). To use this method, firstly, the parameters are defined, namely the values of tolerance and the minimum number of points (Kramer, 2016). In this study, tolerance was set to 5 mm and the minimum points to 50. Then, the algorithm selects an arbitrary point in the dataset and verifies whether it holds the minimum number of points within its neighbourhood. If this condition is met, the point is classified as a central point. This classification process is achieved using a vectorisation approach exclusively for central points, enabling a reduction in the loop overhead in Python runtime (Schubert et al., 2017). This approach proves to be more efficient when utilising the NumPy library (Jones et al., 2001).

For each central point identified, DBSCAN expanded the cluster connected in its reachable neighbourhood. This step is repeated until all reachable points have been included in the cluster. Subsequently, non-central points are evaluated with respect to the constructed clusters. If a non-central point is not close to any neighbourhood, it is deemed as noise and removed. The outcome of this process is a collection of clusters representing the densely connected groups of points in the data space, without the presence of noise points (Stewart and Al-Khassaweneh, 2022).

3.2.6 Leaf, non-leaf, and ground identification

Individual leaf identification implies automatic detection and subsequent removal of leaves from plants. First, parameters are empirically defined, including ranges of RGB values that define the leaves' colours, defined as [0, 10, 0] for minimum RGB (dark green) and [0, 255, 0] for maximum RGB (light green). It also sets a threshold of 80 for the blue component. Then, the cluster is divided into groups, and the mode of the blue component is calculated for each group. If a particular group exceeds the predefined thresholds, filtering is applied to identify the non-leaf objects.

Filtering is performed by calculating the Euclidean distance between the colour of each point and the colour defined as the green threshold for leaves. Points whose distance to the leaf colour is less than a predefined radius (100) and are not white [255, 255, 255] are considered leaves. If the points within the radius of the Euclidean distance meet predefined blue, green, and non-white thresholds, the cluster represents leaves; otherwise, it is categorised as non-leaf. In the experiments performed in this study, many of the non-leaf objects were the targets that were used as Ground Control Points (GCPs).

The process is repeated for all clusters, resulting in a distinction between leaves and non-leaves present in the LiDAR cloud. However, the spectral values of the leaves may be similar to ground values. In this case, the ground points must be removed and identified based on another parameter, such as height (Z component). Therefore, points in the LiDAR cloud that are higher than the proposed threshold for ground points, should be categorised as leaves.

The result of this process is the categorisation of points in the LiDAR cloud into different classes such as leaves, non-leaves and ground points. The cluster of these categories are organised into separate folders to facilitate subsequent analysis and visual interpretation of the data. This approach allows organised information to be categorised based on colour.

4. Results and discussions

4.1 Spectral point cloud generation

4.1.1 Estimation of interior and exterior orientation parameters

Table 1 shows the Interior Orientation Parameters (IOP) estimated by self-calibration in Agisoft Metashape and exported in Australis format. The interior and exterior parameters can be considered similar for images of bands from the same lens. In this paper, one of the six lenses with the 430 nm, 550 nm and 650 nm bands combined in a single sensor lens was used. The IOPs are used to calculate the inverse interior orientation.

IOP	Estimated values	Standard error
f (mm)	21.3437	0.0104
x_0 (mm)	0.2381	0.0085
y_0 (mm)	0.0402	0.0089
K_1 (mm^{-2})	3.24836 e-04	1.65126e-05
K_2 (mm^{-4})	-5.19359e-06	8.67129e-07
K_3 (mm^{-6})	8.20846e-08	1.36101e-08
P_1 (mm^{-1})	-1.09935e-04	3.35188e-06
P_2 (mm^{-1})	-1.36178e-06	3.24654e-06

Table 1 – Estimated interior orientation parameters.

The camera-to-object distance was approximately 1.80 m and the calculated PSOSU (Pixel Size in Object Space Units) for the images was 0.30 mm. The RMSE (Root Mean Square Error) values resulting from the GCPs for the 50 triangulated images correspond to nine times the value of the pixel size in terrain units (Table 2).

It was difficult to obtain better results due to the lack of stable objects in the scene. Nevertheless, the Exterior Orientation Parameters (EOP) obtained from the local coordinates proved to be consistent with the colouring process and with the LiDAR point cloud.

RMSE	
	mm
X	1.59
Y	2.06
Z	1.13
Total	2.84

Table 2 - RMSE of the discrepancies in the GCPs coordinates after triangulation of the 550 nm band images.

4.1.2 Colourisation

The IOPs and EOPs estimated with bundle adjustment were used with the collinearity equations to compute the DN to be assigned to each 3D point, as presented in section 3.2.3. This procedure is repeated for all points visible from each image band. A point cloud of 1,502,161 points was obtained after noise filtering (Figure 2).

The presence of ground points, spheres, and labels is clearly noticeable. Ground points are removed later (Section 4.4), and ground information is reduced due to the MLS noise removal process.

Figure 2 – LiDAR-RGB point cloud, coloured with 430, 550 and 650 nm image bands.

4.2 Removing branches

TLS data was acquired in a single scan from a single station, and, as a consequence, leaf clusters at the trees’ boundaries can store fewer points. In addition, wind can change the position of the leaves during image collection, affecting the filtering step. Thus, determining the appropriate neighbourhood parameter value is important to minimise the effects of outliers on the result (Figure 3).

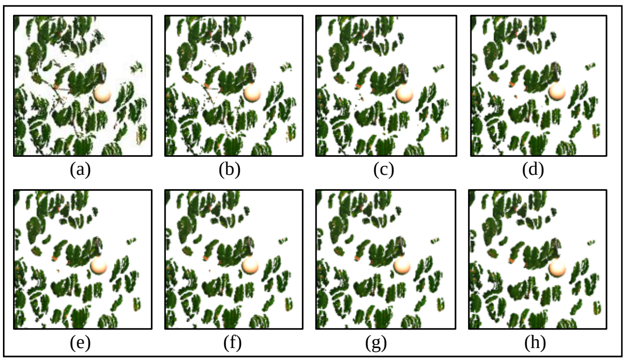

Figure 3 - Original LiDAR-RGB point cloud (a) and with SOR to separate leaves by varying the radius of the neighbourhood: (b) 10, (c) 50, (d) 100, (e) 150, (f) 200, (g) 250, and (h) 300 points.

All points represented as branches are effectively filtered out by the influence radius of 50 (Figure 3.c). However, outliers near the branches could not be removed using the proposed noise removal technique (Section 3.2.2). As a solution, larger radius values (initially up to 300 points) were applied to filter out adjacent noise. This resulted in an undesired removal of some points from the leaf cluster located at the edges. A radius of 250 points was found to be the most suitable for this dataset, removing branches and residual noise without dramatically affecting leaves’ edges.

Leaves near the trees’ boundaries are most affected by SOR point filtering. A complete reconstruction of the leaves would require additional scans from different viewpoints, at the cost of performing accurate registration among all scans.

4.3 Leaf clusters

Leaf, non-leaf, and ground points were satisfactorily detected by DBSCAN. To visualise each cluster created by the algorithm, the bounding boxes in the CloudCompare software can be used. Figure 4 shows the results of two situations that occurred during the clustering process when the leaves were very close to each other.

Separation into clusters was satisfactory in the first case (Figure 4.a). In the second case (Figure 4.b), however, the clustering is not satisfactory since the selected parameters did not segment all leaves separately. The non-leaf and ground points should be filtered to keep only the leaves, either individually or with more than one per cluster.

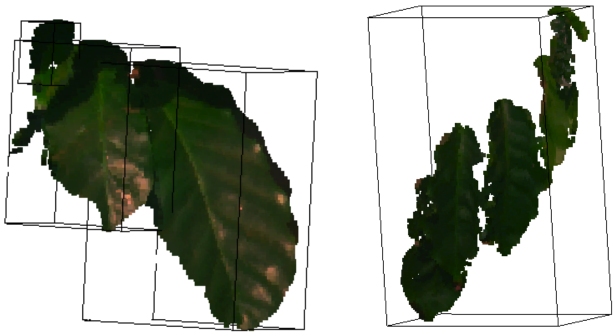

(a) (b)

Figure 4 - Examples of clustering for closely spaced leaves for (a) single leaves and (b) three leaves in a single cluster.

4.4 Clusters after filtering non-leaf objects and ground clusters

It was hypothesised that leaves’ colours would vary in green and blue values. Thus, these two components split leaves from non-leaves. Those clusters that are not within the proposed thresholds are considered as non-leaves, as depicted in Figure 5.

(a) (b) (c) (d)

Figure 5 - Example of identified non-leaves, as (a,d) targets and (b,c) spheres.

Based on the detected clusters, the filtering processes were used to label the clusters as leaves, non-leaves, or ground. Identifying non-leaves using the spectral information only in the full point cloud would be less reliable. This happens because increasing the value of the Euclidean distance delineates well the non-leaves points farther from the cloud, but non-leaves near the leaves are not identified. After segmenting the point cloud, some non-leaves were removed using spectral information (Figure 6).

(a) (b)

Figure 6 - (a) Non-leaves and leaf clusters and (b) points in black were filtered.

https://doi.org/10.5194/isprs-annals-X-3-2024-269-2024

Labelling leaves is more efficient and less computationally expensive when performing the operation directly on the cluster. Some leaf points are still filtered but to a lesser degree. After filtering the non-leaves, the ground clusters were still counted along with the other leaf clusters since some ground points and leaves had similar colours. In this case, a threshold for points' heights was defined empirically. Leaf clusters are shown in Figure 7, and metrics are discussed in 4.5.

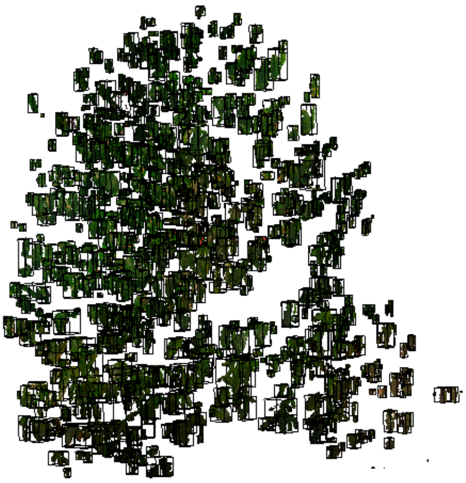

Figure 7 - Clusters labelled as leaves only.

4.5 Discussions

The plot presented in Figure 8 shows the total number of points after the filtering with the SOR technique against the neighbourhood points used for this filtering. It was observed that a large radius of influence from the neighbourhood is unnecessary to remove the cluster of branch-like points, as discussed in Section 4.2 but some neighbourhood noise still exists. Increasing the size of the neighbourhood will result in a stronger filtering of the subsequent points, which will primarily affect the leaves at the edges of the point cloud, as previously mentioned.

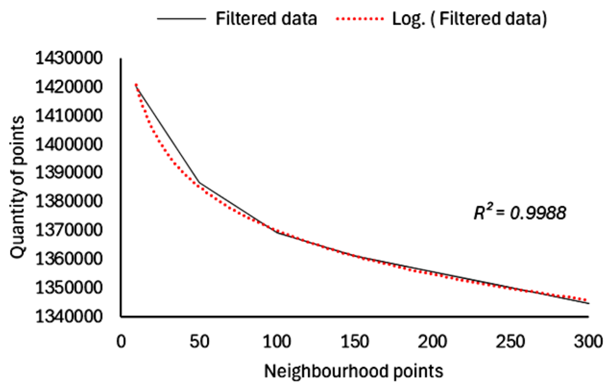

Figure 8 - Number of points after filtering for each neighbourhood value.

The best fit to the data presented in Fig. 8 is a logarithmic model with a high R^2 value. Changing the parameter (number of neighbours) has a significant initial effect on the filtering. As the filtering progresses, with a higher number of neighbours, changes become less noticeable. This attenuation is due to the increase in the density of the points in the clusters as the neighbourhood value increases, and noise near the branches still exists despite the preprocessing noise filtering. The stabilisation of the filtering process suggests the elimination of outliers only, thereby eliminating the need for point densification in the final result. In contrast to methods such as DoN, Li et al. (2020) observed a significant reduction in the number of leaf points. When we applied DoN to this dataset, the reduction was significant enough to potentially affect leaf characterisation.

A total of 1,226 clusters containing leaves, non-leaves, and ground points were then generated by the DBSCAN technique. The points from the point cloud labelled as non-leaves were initially used in the colourisation process. However, to achieve only the leaves in the final result, these objects needed to be subsequently removed in the process. Identification errors (Table 3) resulted from the filtering techniques used to label the scene and were observed through visual inspection.

Identification	**Correct**	**Incorrect**	**Total**
Leaves	1,109 (99.2%)	9 (0.8%)	1,118
Non-leaves	7 (100%)	0 (0%)	7
Ground	97 (96¨%)	4 (4%)	101
Total	1,213 (98.9%)	13 (1.1%)	1,226

Table 3 - Correct and incorrect identification for clusters.

In some cases, leaves were labelled as non-leaves mainly when they were wrongly segmented with other non-leaves objects. In some cases, the error was caused by leaf's specular reflection producing high blue values, exceeding the proposed threshold. Although ground clusters included points close to the leaves, the height (Z) threshold was maintained. The technique gave a satisfactory result of 98.9% accuracy in identifying and labelling the segmented objects.

5. Conclusions

In this study, we developed a method for leaf detection in high-density terrestrial LiDAR data. The process entails branch filtering, segmentation, and leaf identification. Initially, we employed a noise removal technique inspired by MLS and assigned RGB colours to the points. Subsequently, branch filtering was performed using the SOR filter, and similar points were segmented using the DBSCAN method. Finally, leaf identification was conducted based on RGB values, and ground points were filtered based on maximum height.

Implementing the SOR method for branch and leaf separation has proven effective in filtering out points defined as branches in high-density LiDAR-RGB. This technique reduces the need for additional leaf densification procedures since only the smallest clusters of points, such as branches, noise, and partially scanned leaves in the collection, are affected.

Although the existing clustering technique shows positive results in the context of point clouds with low canopy density and indoors (Liu et al., 2020), the detection of individual leaves with the supervised DBSCAN method proved to be efficient for semantic segmentation in trees with a high canopy density. However, its performance was less optimal compared to trees with low canopy density. Separating the leaves individually will assist in the labelling stage, avoiding incorrectly labelling as a single non-leaf when the cluster contains both leaves and non-leaves objects. In the existing literature, it is noted that these methods have not been explored in the context of trees with high leaf density. Typically, individual leaf separation is addressed in trees with low leaf density, thus remaining a challenge to be overcome in precision agriculture.

For future work, it is suggested refining the DBSCAN parameters. In this regard, it is recommended to implement other instance segmentation (individual leaf) methods. This includes considering additional descriptive leaf characteristics, such as normal or curvature, beyond Euclidean distance. The detection of individual leaves enables applications for calculating the maximum length of the leaf, width, inclination, and number of leaves. Furthermore, it is recommended to extend the colourisation process to other bands of the multispectral camera to extract additional radiometric attributes.

Acknowledgements

This study was financed in part by the Coordenação de Aperfeiçoamento de Pessoal de Nível Superior – Brasil (CAPES) (Grants: 88887.961781/2024-00, 88887.821780/2023-00, 88887.310313/2018-00, 88887.898553/2023-00), by the National Council for Scientific and Technological Development, CNPq (Grants: 130414/2022-0, 303670/2018-5, 308747/2021-6) and by the São Paulo Research Foundation, FAPESP (Grants: 2021/06029-7, 2023/14756-1).

References

Agrowing Development Team. 2024. Agrowing - Advanced Agricultural Solutions. Available online: https://agrowing.com/ (accessed on 20 January 2024)..

Ao, Z.; Wu, F.; Hu, S.; Sun, Y.; Su, Y.; Guo, Q.; Xin, Q. 2022. Automatic segmentation of stem and leaf components and individual maize plants in field terrestrial LiDAR data using convolutional neural networks. *The Crop Journal* 10: 1239–1250.

Appel, A. 1968. Some techniques for shading machine renderings of solids. *Proc. of the SJCC*: 37–45.

Assarsson, U.; Moller, T. 2000. Optimized view frustum culling algorithms for bounding boxes. *J. Graph. Tools*, 5: 9–22.

Blinn, J.F. 1993. Backface culling snags (rendering algorithm). *IEEE Comput. Graph. Appl.,* 13: 94–97.

Catmull, E.E. 1974. A subdivision algorithm for computer display of curved surfaces. *World Journal of Mechanics*.

Cohen-Or, D.; Chrysanthou, Y.L.; Silva, C.T.; Durand, F. 2003. A survey of visibility for walkthrough applications. *IEEE Trans. Vis. Comput. Graph.,* 9: 412–431.

Costa, C.; Schurr, U.; Loreto, F.; Menesatti, P.; Carpentier, S. 2019. Plant phenotyping research trends, a science mapping approach. *Front. Plant Sci.,* 9: 426195.

Crombez, N.; Caron, G.; Mouaddib, E. 2015. 3D point cloud model colorization by dense registration of digital images. *Int. Arch. Photogramm. Remote Sens. Spatial Inf. Sci.,* 40: 123–130.

Deng, D. 2020. DBSCAN Clustering Algorithm Based on Density. *Proc. IFEEA 2020,* 949–953.

Dorj, U.-O.; Lee, M.; Yun, S. 2017. An yield estimation in citrus orchards via fruit detection and counting using image processing. *Computers and electronics in agriculture* 140: 103–112.

Ester, M.; Kriegel, H.P.; Sander, J.; Xu, X. 1996. A density-based algorithm for discovering clusters in large spatial databases with noise. *kdd*, 226–231p.

Fuchs, H.; Kedem, Z.M.; Naylor, B.F. 1980. On visible surface generation by a priori tree structures. *Proc. SIGGRAPH*: 124–133.

Gomes, D.P.S.; Zheng, L. 2020. Leaf segmentation and counting with deep learning: on model certainty, test-time augmentation, trade-offs. *arXiv preprint arXiv:2012.11486*.

Hu, F.; Lin, C.; Peng, J.; Wang, J.; Zhai, R. 2022. Rapeseed leaf estimation methods at field scale by using terrestrial LiDAR point cloud. *Agronomy* 12: 2409.

Huang, H.; Yan, X.; Yang, J.; Cao, Y.; Zhang, X. 2023. Lidsor: a Filter for Removing Rain and Snow Noise Points from LIDAR Point Clouds in Rainy and Snowy Weather. *The International Archives of the Photogrammetry, Remote Sensing and Spatial Information Sciences* 48: 733–740.

Jenke, P.; Wand, M.; Bokeloh, M.; Schilling, A.; Straßer, W. 2006. Bayesian Point Cloud Reconstruction. *Computer Graphics Forum* 25: 379–388.

Jimenez-Berni, J.A.; Deery, D.M.; Rozas-Larraondo, P.; Condon, A.T.G.; Rebetzke, G.J.; James, R.A.; et al. 2018. High throughput determination of plant height, ground cover, and above-ground biomass in wheat with LiDAR. *Frontiers in plant science* 9: 335148.

Jin, S.; Su, Y.; Wu, F.; Pang, S.; Gao, S.; Hu, T.; et al. 2018. Stem–leaf segmentation and phenotypic trait extraction of individual maize using terrestrial LiDAR data. *IEEE Transactions on Geoscience and Remote Sensing* 57: 1336–1346.

Jones, E.; Oliphant, T.; Peterson, P. 2001. SciPy: Open source scientific tools for Python. https://www.scipy.org.

Katz, S.; Tal, A.; Basri, R. 2007. Direct visibility of point sets. *ACM SIGGRAPH 2007 papers*: 24-es.

Khan, K.; Rehman, S.U.; Aziz, K.; Fong, S.; Sarasvady, S. 2014. DBSCAN: Past, present and future. *The fifth international conference on the applications of digital information and web technologies (ICADIWT 2014)*: 232–238.

Kramer, O. 2016. *Machine learning for evolution strategies*. Vol. 20. Springer, .

Li, D.; Cao, Y.; Tang, X.-S.; Yan, S.; Cai, X. 2018. Leaf Segmentation on Dense Plant Point Clouds with Facet Region Growing. *Sensors (Basel, Switzerland)* 18: 3625.

Li, D.; Shi, G.; Kong, W.; Wang, S.; Chen, Y. 2020. A leaf segmentation and phenotypic feature extraction framework for multiview stereo plant point clouds. *IEEE Journal of Selected Topics in Applied Earth Observations and Remote Sensing* 13: 2321–2336.

Li, S.; Dai, L.; Wang, H.; Wang, Y.; He, Z.; Lin, S. 2017. Estimating leaf area density of individual trees using the point cloud segmentation of terrestrial LiDAR data and a voxel-based model. *Remote Sensing* 9: 1202.

Li, Z.; Wang, J.; Zhang, Z.; Jin, F.; Yang, J.; Sun, W.; et al. 2022. A Method Based on Improved IForest for Trunk Extraction and Denoising of Individual Street Trees. *Remote Sensing* 15: 115.

Liu, X.; Hu, C.; Li, P. 2020. Automatic segmentation of overlapped poplar seedling leaves combining Mask R-CNN and DBSCAN. *Computers and Electronics in Agriculture* 178: 105753.

Liu, Z.; Song, S.; Wang, B.; Gong, W.; Ran, Y.; Hou, X.; et al. 2022. Multispectral LiDAR point cloud highlight removal based on color information. *Optics Express* 30: 28614–28631.

Masuda, T. 2021. Leaf Area Estimation by Semantic Segmentation of Point Cloud of Tomato Plants. *2021 IEEE/CVF International Conference on Computer Vision Workshops (ICCVW)*: 1381–1389.

Pedregosa, F.; Varoquaux, G.; Gramfort, A.; Michel, V.; Thirion, B.; Grisel, O.; et al. 2011. Scikit-learn: Machine learning in Python. *The Journal of machine Learning research* 12: 2825–2830.

Rusu, R.B.; Cousins, S. 2011. 3D is here: Point Cloud Library (PCL). *2011 IEEE International Conference on Robotics and Automation*: 1–4.

Schall, O.; Belyaev, A.; Seidel, H.-P. 2005. Robust filtering of noisy scattered point data. *Proceedings Eurographics/IEEE VGTC Symposium Point-Based Graphics, 2005.*: 71–144.

Schubert, E.; Sander, J.; Ester, M.; Kriegel, H.P.; Xu, X. 2017. DBSCAN revisited, revisited: why and how you should (still) use DBSCAN. *ACM Transactions on Database Systems (TODS)* 42: 1–21.

Seitz, S.M.; Dyer, C.R. 1999. Photorealistic Scene Reconstruction by Voxel Coloring. *International Journal of Computer Vision* 35: 151–173.

Stewart, G.; Al-Khassaweneh, M. 2022. An implementation of the HDBSCAN* clustering algorithm. *Applied Sciences* 12: 2405.

Tommaselli, A.M.G.; Berveglieri, A.; Imai, N.N.; Santos, G.H.; Moriya, E.A.S.; Watanabe, F.S.Y.; Salvador Neto, L. 2020. Geometric performance of a camera with single sensor and multiple heads. *The International Archives of Photogrammetry, Remote Sensing and Spatial Information Sciences* 43: 389–396.

Wan, P.; Shao, J.; Jin, S.; Wang, T.; Yang, S.; Yan, G.; et al. 2021. A novel and efficient method for wood–leaf separation from terrestrial laser scanning point clouds at the forest plot level. *Methods in ecology and evolution* 12: 2473–2486.

Whitted, T. 1979. An improved illumination model for shaded display. *Proceedings of the 6th annual conference on Computer graphics and interactive techniques*: 14.

Xie, Z.; Lang, Y.; Chen, L. 2021. Geometric modeling of Rosa roxburghii fruit based on three-dimensional point cloud reconstruction. *Journal of Food Quality* 2021: 1–14.

Zhang, Z. 1994. Iterative point matching for registration of free-form curves and surfaces. *International journal of computer vision* 13: 119–152.

Zhou, J.; Wei, H.; Zhou, G.; Song, L. 2019. Separating leaf and wood points in terrestrial laser scanning data using multiple optimal scales. *Sensors* 19: 1852.